



# OPEN Study on constitutive model of marine soft soil based on disturbed state concept

Heng Zhang<sup>1</sup>, Yindong Sun<sup>1</sup>, Yajun Liu<sup>1</sup>, Ke Wu<sup>1✉</sup>, Yang Zheng<sup>1</sup>, Haijun Lu<sup>2</sup> & Rong Chen<sup>3</sup>

Marine soft soils are widely distributed in near-coastal areas and pose significant risks to the stability of structures due to their unique mechanical properties. While researchers worldwide have used various theoretical constitutive models and scientific methods to investigate the mechanical properties of marine soft soils, no attempts have been made to establish a mechanical model based on the concept of disturbed state for marine soft soils. In this paper, based on the concept of disturbed state, we utilize triaxial and creep test methods, apply the Duncan tensor modulus to describe the relatively complete state of marine soft soil, and modify the Cambridge model to characterize the fully adjusted state. Additionally, we derive the disturbance function to establish the intrinsic model for the disturbed state of marine soft soil. The model's accuracy is verified by comparing its predictions with experimental test results. Subsequently, the model is applied to engineering cases and compared with numerical simulation results. The study shows that the results from the disturbed state constitutive model are consistent with the experimental data and can effectively be used to assess the foundation bearing capacity of marine soft soil layers. The development of the constitutive model based on the concept of disturbed state offers a new theoretical framework and calculation method for studying the mechanical properties of marine soft soil in near-coastal regions.

**Keywords** Disturbed state concept, Marine soft soil, Constitutive model, Geotechnical tests, Numerical calculation

Marine soft soil is a type of weak soil formed through deposition in marine environments, commonly found in near-coastal areas. It exhibits complex physical properties, characterized by high moisture content, significant organic matter, large compressibility, and low shear strength. Additionally, marine soft soil possesses structural characteristics, such as the interaction and arrangement of particles, which significantly influence its engineering properties. Due to these inherent characteristics, marine-phase soft soils pose several challenges in near-coastal engineering, including uneven settlement of marine foundations, landslides on coastal slopes, and deformation and instability in tunneling projects<sup>1–3</sup>. Consequently, understanding the mechanical properties of marine-phase soft soil is crucial for predicting and controlling the long-term stability of engineering structures in near-coastal regions.

The study of the mechanical properties of marine soft soil primarily employs indoor triaxial tests, theoretical analysis, and numerical simulation methods. A key aspect of this research is the selection and development of an intrinsic model for marine soft soil, which directly influences the accuracy of the soil's mechanical property characterization. The intrinsic model serves as a mathematical representation of the stress-strain relationship of marine soft soil, aiming to capture its deformation and strength characteristics. Currently, the principal constitutive models for marine soft soil include the nonlinear elastic, elastic-plastic, damage mechanics, and disturbance state models. In the case of the nonlinear elastic model, the stress-strain relationship is derived by fitting experimental data to an existing empirical formula. This model assumes that the soil undergoes fully recoverable strains following compression, with a nonlinear stress-strain behavior. The elastic-plastic model accounts for both recoverable elastic strain and irrecoverable plastic strain, reflecting the mechanical response of the soil as an elastic-plastic material under compression. This model more accurately captures the soil's mechanical properties based on material tests. The damage mechanics model uses a damage variable to describe the process by which the original structural clay loses strength and gradually transitions into remolded soil. In this model, strain is chosen as a parameter for the damage variable, and the theory of composite material damage mechanics is applied to establish the constitutive model for structural clay<sup>4</sup>. These three types of constitutive models are widely referenced in studies of the mechanical properties of marine soft soil. A constitutive model is presented for clay soils subjected to cyclic loading with entrained

<sup>1</sup>School of Civil Engineering, Shandong University, Jinan 250061, China. <sup>2</sup>School of Civil Engineering and Architecture, Wuhan Polytechnic University, Wuhan 430023, China. <sup>3</sup>Institute of Geotechnical Engineering, Northeast Electric Power University, Jilin 132012, China. ✉email: wuke@sdu.edu.cn

gas bubbles under undrained and ungasged conditions. This model extends the boundary surface model developed by Huang et al. for fine-grained saturated soils, incorporating gas effects such as changes in soil volume due to gas compression and the plastic modulus associated with pore pressure<sup>5</sup>. A fractional-order elastic-plastic constitutive model for marine silt is proposed, combining the modified Cam-clay model with fractional-order calculus. This model captures key properties of marine silt, including shear shrinkage, friction, and stress-history dependence<sup>6</sup>. An incremental three-dimensional Nishihara model is introduced to describe the stress-strain behavior of soft soils. The transversely isotropic viscoelastic-viscoplastic damage constitutive equations for soils are derived by applying the Drucker-Prager yield criterion for transversely isotropic media, incorporating the transversely isotropic flexibility matrix and the damage law of the Nishihara model<sup>7</sup>. A numerical implementation of the SANICLAY model, which accounts for the structural properties of clays, is developed with submarine primary soils as the focus. This structural multi-yield-surface model is applied to finite element analysis through the sub-incremental step-explicit algorithm and secondary finite element development<sup>8</sup>. A state-dependent critical state model, which describes the different behaviors of air-bearing sands under various states, is proposed and implemented in ABAQUS to simulate the stability of submarine slopes under undrained loading conditions<sup>9</sup>. The stabilization mechanisms of cement and glass fibers are explored through damage analysis and microscopic observations. Based on these findings, a damage constitutive model for FCSSC is formulated, and the model's validity is confirmed by comparing the fitted curves to experimental data<sup>10</sup>. Finally, thermally induced strains and creep strain rates under varying temperature paths are examined. A novel one-dimensional thermoelastic-viscoplastic model is developed, extending an existing 1D elastic-viscoplastic framework<sup>11</sup>. The disturbed state principal model was established by the renowned American scholar Prof. C.S. Desai in 1974<sup>12</sup>. This theory integrates the mechanical principles of elasticity, plasticity, and viscoplasticity, while also incorporating elements of damage mechanics, critical state theory, and self-organized criticality<sup>13</sup>. Currently, both domestic and international researchers focus on developing disturbed state isomorphic models for materials in various fields based on this theory, achieving significant advancements and satisfactory results. By analyzing the results of triaxial compression tests, a new disturbance function related to the bulk modulus and shear modulus parameters was developed, and the evolution of this disturbance function was investigated<sup>14</sup>. A constitutive model for uniaxial strain softening in fiber-reinforced soils was formulated using the Disturbed State Concept (DSC). The model incorporates five essential parameters that vary with fiber content, and five sets of uniaxial compression test data for different fiber-reinforced soils were evaluated<sup>15</sup>. Nonlinearities arising from variations in material properties, soil thickness, and creep behavior are considered. The relationship between the soil state during consolidation and its relatively intact and fully adjusted states is characterized by two consolidation and creep state functions<sup>16</sup>. Additionally, an improved Duncan-Chang model was proposed to account for the impact of disturbance on the strength-deformation characteristics of sandy pebble soils, establishing the relationship between the initial tangent modulus, peak strength, and relative compactness parameters<sup>17</sup>.

It is evident that the constitutive models based on the concept of the disturbed state encompass a wide range of geotechnical materials; however, there has been limited research specifically addressing the constitutive modeling of marine soft soil. Therefore, this paper proposes a constitutive model for marine soft soil based on the disturbed state concept. The Duncan tensor modulus is employed to represent the relatively intact state of marine soft soil, while the modified Cambridge model is used to describe the fully adjusted state. Additionally, a disturbance function is derived from creep test results to establish the intrinsic model of the disturbed state for marine soft soil. This model is validated through relevant testing and applied in engineering case studies. The proposed approach provides an accurate and effective constitutive model and research methodology for studying the mechanical properties of marine soft soil.

## Constitutive model for the disturbed state of marine soft soil

Desai conducted research on the structural properties of soil, leading to the development of the Disturbed State Concept (DSC). This theory assumes that the material exists in two states: the perfect relative integrity state and the fully adjusted state of complete disturbance. Any disturbance of the material's state lies between these two reference states, and the transition from the initial state to another is described by a disturbance function (also known as the disturbance factor). The significance of DSC lies in its use of these two reference states within the constitutive model, allowing for a more accurate description of the material's true behavior. This approach combines the strengths of both states while avoiding their individual shortcomings. However, the effectiveness of this theory depends on selecting an appropriate constitutive model to describe these two reference states, as well as using a disturbance function that accurately captures the transformation relationship and the evolution of these states. Only when these two conditions are met can the desired results be achieved<sup>12,13</sup>.

### Basic assumptions

To establish the disturbed state constitutive model for marine soft soil, the following assumptions are made:

- (1) The material of marine soft soil is considered macroscopically homogeneous and isotropic.
- (2) The direction of the plastic strain increment coincides with the direction of the plastic stress increment, meaning that the rotation of the principal stress axes is neglected.
- (3) The soil in a fully adjusted state, which has undergone a certain level of hydrostatic pressure, can continue to withstand a specific shear stress.
- (4) The direction of plastic flow is assumed to coincide with the direction of plastic loading, following the correlation-linked orthogonal flow rule.
- (5) The mechanical properties of the fully adjusted state soil are assumed to be similar to those of remolded soil.

### Relatively intact state constitutive model

The nonlinear elastic model is commonly used in geotechnical structural analysis due to its ability to effectively simulate the rheological properties of soft soils while maintaining a simple structure. As a result, the Duncan-Zhang model is adopted for the relatively complete state principal model. This model accounts for both nonlinear and elastic-plastic behavior of the soil during loading and unloading. The stress-strain relationship for this model is given by:

$$\sigma_1 = \sigma_3 + K \cdot (\sigma_3^n) \cdot \left( \frac{\epsilon_1}{1 + R_f \cdot \frac{\epsilon_1}{\epsilon_f}} \right) \quad (1)$$

where  $\sigma_1$  and  $\sigma_3$  are the maximum and minimum principal stresses, respectively;  $\epsilon_1$  is the axial strain;  $K$  is the initial modulus of elasticity-related parameter, obtained by fitting experimental data;  $n$  is the material's degree of nonlinearity parameter, also determined from experimental data;  $R_f$  is the ratio of destructive stresses, typically determined experimentally, and is generally taken as a value between 0 and 1;  $\epsilon_f$  is the strain at failure, which is determined from experimental data.

Differentiating Eq. (1) yields:

$$\frac{d\sigma_1}{d\epsilon_1} = K \cdot (\sigma_3^n) \cdot \frac{\epsilon_f}{(\epsilon_f + R_f \cdot \epsilon_1)^2} \quad (2)$$

This results in an expression for the axial strain increment in the relatively complete state Duncan tensor model:

$$d\epsilon_1^i = \frac{d\sigma_1}{K \cdot (\sigma_3^n) \cdot \frac{\epsilon_f}{(\epsilon_f + R_f \cdot \epsilon_1)^2}} \quad (3)$$

In the Duncan-Zhang model, the calculation of the incremental volumetric strain ( $\epsilon_v$ ) is directly related to the incremental axial and radial strains. The volumetric strain ( $\epsilon_v$ ) is the sum of the axial strain ( $\epsilon_1$ ) and twice the radial strain ( $\epsilon_3$ ), i.e.,  $\epsilon_v = \epsilon_1 + 2\epsilon_3$ . Therefore, its incremental expression can also be derived from the increments of these two strains.

Assuming that the marine soft soil is isotropic, the radial strain increment can be expressed in terms of Poisson's ratio ( $\nu$ ). This is because the axial stress increment influences the radial strain in a three-dimensional stress state. The resulting mathematical expression for the volumetric strain increment is:

$$d\epsilon_v^i = (1 - 2\nu) \cdot \frac{d\sigma_1}{E_t} \quad (4)$$

where  $E_t$  is the tangent modulus calculated in the Duncan tensor model, and  $\nu$  is the Poisson's ratio, which must be determined experimentally.

The expression for shear stress in the Duncan-Zhang model is:

$$\epsilon_s = \frac{\tau}{G} \quad (5)$$

Where  $\tau$  is the shear stress,  $\epsilon_s$  is the shear strain, and  $G$  is the shear modulus, which is expressed as  $G = E/2(1 + \nu)$ .

The resulting mathematical expression for the shear strain increment in the relatively complete state Duncan tensor model is:

$$d\epsilon_s^i = \frac{d\tau}{G} \quad (6)$$

where the expression for  $d\tau$  is:

$$d\tau = d\sigma' \tan \left[ \varphi' + \psi \left( \frac{p'}{p'_a} \right)^\beta \right] + \sigma' \sec^2 \left[ \varphi' + \psi \left( \frac{p'}{p'_a} \right)^\beta \right] \psi \beta \left( \frac{p'}{p'_a} \right)^{\beta-1} \frac{dp'}{p'_a} \quad (7)$$

where  $\sigma'$  is the effective positive stress,  $\varphi'$  is the effective friction angle,  $\psi$  is a parameter in the Duncan-Zhang model representing the increment of the friction angle,  $p'$  is the effective circumferential pressure,  $p'_a$  is referring to atmospheric pressure (typically used as the reference pressure), and  $\beta$  is a model parameter that influences the degree of pressure dependence.

In summary, the incremental matrix equation can be expressed as:

$$\begin{bmatrix} d\epsilon_v^i \\ d\epsilon_s^i \end{bmatrix} = \begin{bmatrix} D_{vv} & D_{vq} \\ D_{qv} & D_{qq} \end{bmatrix} \begin{bmatrix} dp' \\ dq \end{bmatrix} \quad (8)$$

where  $D_{vv}$  is usually expressed as  $1/K$ , reflecting the sensitivity of the volumetric strain to changes in the mean effective stress, and  $K$  can be obtained from the equivalent volumetric strain-mean stress relationship;  $D_{vq}$  may be zero or a very small value, reflecting the dependence of the volumetric strain on changes in the bias stress;  $D_{qv}$  may be zero or very small as well, reflecting the dependence of the shear strain on the changes in the mean effective stress;  $D_{qq}$  is  $1/G$ , reflecting the sensitivity of the shear strain to changes in the bias stress.

### Fully adjusted state constitutive model

The concept of disturbance state theory suggests that after a material is subjected to external loads, this disturbance causes the material to spontaneously, consciously, and automatically adjust to another stable state in response to the external forces. This new state is referred to as the fully adjusted state, which represents the limiting condition of geotechnical materials after they have been subjected to stresses. Materials in the fully adjusted state are typically characterized by one of the following three state models:

- (1) The material lacks any strength, similar to the behavior of pores in the damage model of a continuous medium<sup>18</sup>.
- (2) The material has no shear strength but can withstand hydrostatic pressure, akin to a constrained liquid.
- (3) The material can resist shear stress under a certain level of hydrostatic pressure, i.e., it has shear strength and can reach a critical state. At this point, only shear strain occurs, and no volumetric strain is observed, making it similar to a liquid-solid mixture under constraint<sup>15</sup>.

However, unlike general solid materials, soil, as a special type of porous medium, not only undergoes shear strain but also experiences significant volumetric strain during the stressing process. Therefore, the fully adjusted state of soil must consider both shear and volumetric strains to accurately reflect the mechanical properties of geotechnical materials. In general, the fully adjusted state can be described using elastic, plastic, or elastoplastic models<sup>19</sup>.

According to the theory of superstress rheology proposed by Perzyna, the visco-plastic strain rate  $\dot{\gamma}_{vm}^{vp}$  is denoted as:

$$\dot{\gamma}_{vm}^{vp} = S \frac{\partial F}{\partial \sigma'_{ij}} \quad (9)$$

where  $\dot{\gamma}_{vm}^{vp}$  is the viscoplastic strain rate tensor;  $S$  is the viscoplastic scaling factor, which is used to express the viscoplastic strain rate  $\dot{\gamma}_{vm}^{vp}$  is the magnitude of the viscoplastic strain rate tensor;  $\sigma'_{ij}$  is the effective stress tensor;  $\frac{\partial F}{\partial \sigma'_{ij}}$  is the direction used in the plastic flow law to determine the viscoplastic strain rate, and  $F$  is the visco-plasticity function, which is also known as the yield surface function<sup>20</sup>.

For this reason, in this paper, the critical state theory is selected to describe the mechanical behavior of the fully adjusted state. Specifically, the modified Cambridge model is used to represent the remolded soil, and the yield surface equation is given by:

$$F = p' \left( 1 + \frac{q^2}{M^2 p'^2} \right) - p'_0 = 0 \quad (10)$$

where  $p'$  is the average effective stress,  $q$  is the deviatoric stress,  $p'_0$  is the effective value of the vertical stress ( $p_0$ ) in the initial stress field, and  $M$  is the slope of the critical state line for the soil. From this, the mathematical expression for the strain of the modified Cambridge model in the fully adjusted state can be derived as:

$$\epsilon_v^c = \lambda \ln \left( \frac{p}{p_0} \right) + \kappa \ln \left( \frac{p' + p}{p'_0 + p_0} \right) \quad (11)$$

The resulting expression for the strain increment of the modified Cambridge model in the fully adjusted state is given by:

$$d\epsilon_v^c = d\epsilon_v^e + d\epsilon_v^p = \kappa \frac{dp'}{p'} + \frac{(1 + e_0)(dp + dq)}{(\lambda - \kappa)} \quad (12)$$

where  $e_0$  is the initial pore ratio,  $dp$  is the increment of the effective mean stress, and  $dq$  is the increment of the shear stress.

The mathematical expression for the shear strain in the modified Cambridge model for the fully adjusted state can be written as:

$$\epsilon_s^c = \frac{q}{G} \quad (13)$$

where  $G$  is the shear modulus, which can either be a constant or a variable dependent on the state of the soil (e.g., effective stress, pore ratio), and is given by  $G = \frac{1+e_0}{2(1-2\nu)} K$ . Additionally, in the modified Cambridge model, the plastic potential function is often assumed to be a straight line parallel to the critical state line, with the equation is  $q = Mp'$ .

The resulting expression for the shear strain increment in the modified Cambridge model for the fully adjusted state is:

$$d\epsilon_s^c = \frac{1+v}{E} dq + \frac{dq}{M^2(p+p')} \quad (14)$$

where the parameter  $M$  is calculated by the following equation:

$$M = \frac{6\sin\phi'}{3 - \sin\phi'} \quad (15)$$

where  $\phi'$  is the angle of internal friction for marine soft soils.

The parameters  $\lambda$  and  $\kappa$  can be derived from the side-limit compression test using the following equations:

$$\lambda = C_c/2.303 \quad (16)$$

$$\kappa = C_s/2.303 \quad (17)$$

where  $C_c$  and  $C_s$  are the compression and resilience indices of the remolded soil in the  $e$ - $\lg p$  plane, respectively<sup>19</sup>.

In summary, the incremental matrix equation for the modified Cambridge model in the fully adjusted state can be expressed as:

$$\begin{bmatrix} d\epsilon_v^c \\ d\epsilon_s^c \end{bmatrix} = \begin{bmatrix} (\lambda - \kappa) \frac{1}{p'} & 0 \\ 0 & \frac{1}{G} \end{bmatrix} \begin{bmatrix} dp' \\ dq \end{bmatrix} \quad (18)$$

### Disturbed function

Through the disturbance function, the dynamic processes occurring within the microstructure of the material under external forces can be expressed in terms of its macroscopic response. This approach avoids the complexity associated with the microscopic study of the material's mechanical properties. The general expression for the disturbance function was proposed by C.S. Desai:

$$\begin{cases} D_v = 1 - \exp(-A_v \epsilon_v^{Z_v}) \\ D_s = 1 - \exp(-A_s \epsilon_s^{Z_s}) \end{cases} \quad (19)$$

where  $D_v$  and  $D_s$  are the disturbance functions of body strain and shear strain, respectively, and  $A_v$ ,  $Z_v$ ,  $A_s$ , and  $Z_s$  are the test parameters. Where,  $D_v$ ,  $D_s$  can be calculated by the following two Eqs.<sup>18,20</sup>:

$$\begin{cases} D_v = \frac{\epsilon_v^i - \epsilon_v^a}{\epsilon_v^i - \epsilon_v^c} \\ D_s = \frac{\epsilon_s^i - \epsilon_s^a}{\epsilon_s^i - \epsilon_s^c} \end{cases} \quad (20)$$

where the superscripts  $i$ ,  $a$ , and  $c$  represent the relatively complete state, the actual state, and the fully adjusted state, respectively.

$D_v$  can be derived from isotropic consolidation creep tests:

$$\begin{cases} \epsilon_v^i = e_0 - \kappa^i \ln p' \\ \epsilon_v^c = e_0 - (\lambda^0 - \kappa^c) \ln p_s - \kappa^c \ln p' \end{cases} \quad (21)$$

where  $e_0$  is the initial pore ratio of the marine phase soft soil in its natural state.

$D_s$  can be obtained from triaxial consolidation undrained creep tests. The relative complete state  $\epsilon^i$  and the fully adjusted state  $\epsilon^c$  can be determined by integrating Eq. (8) and Eq. (18), while considering the initial conditions.

### Constitutive model of marine soft soil based on disturbance state

Based on the disturbed state theory, the conceptual incremental equation for the disturbed state of marine soft soil is given by:

$$d\epsilon_{ij} = (1 - D_\epsilon) d\epsilon_{ij}^i + D_\epsilon d\epsilon_{ij}^c + dD_\epsilon (\epsilon_{ij}^c - \epsilon_{ij}^i) \quad (22)$$

where  $\epsilon_{ij}$  is the actual observed strain tensor;  $\epsilon_{ij}^i$  is the strain tensor for the relatively complete state;  $\epsilon_{ij}^c$  is the strain tensor for the fully adjusted state;  $D_\epsilon$  is the disturbance function. The resulting matrix expressions for the body strain increment and the bias strain increment can be obtained:

$$\begin{bmatrix} d\epsilon_v \\ d\epsilon_s \end{bmatrix} = \begin{bmatrix} 1 - D_v & D_v \\ 1 - D_s & D_s \end{bmatrix} \begin{bmatrix} d\epsilon_v^i - \epsilon_v^i \\ d\epsilon_s^i - \epsilon_s^i \\ d\epsilon_s^c - \epsilon_s^c \end{bmatrix} = \begin{bmatrix} 1 - D_v & D_v \\ 1 - D_s & D_s \end{bmatrix} \begin{bmatrix} (D_{11}^c - D_{11}^i) + ((D_{12}^c - D_{12}^i) \frac{D_{11}^i + D_{12}^i}{D_{11}^c + D_{12}^c}) \\ (D_{21}^c - D_{21}^i) + ((D_{22}^c - D_{22}^i) \frac{D_{21}^i + D_{22}^i}{D_{21}^c + D_{22}^c}) \\ (D_{21}^c - D_{21}^i) + ((D_{22}^c - D_{22}^i) \frac{D_{21}^i + D_{22}^i}{D_{21}^c + D_{22}^c}) \end{bmatrix} \begin{bmatrix} dp' \\ dq \end{bmatrix} \quad (23)$$

where,

$$D^i = \begin{bmatrix} D_{vv} & D_{vq} \\ D_{qv} & D_{qq} \end{bmatrix} \quad (25)$$

$$D^c = \begin{bmatrix} (\lambda - \kappa) \frac{1}{p'} & 0 \\ 0 & \frac{1}{G} \end{bmatrix} \quad (25)$$

### Constitutive model program of the disturbed state of marine soft soil

The program implementation of the disturbed state constitutive model for marine-phase soft soil is based on modeling the stress-strain relationship of marine-phase soft soil under different loading states. Specifically, the Duncan-Zhang model and the modified Cambridge model are used, while simultaneously calculating the disturbance effect on the soil body. To achieve this, the paper adopts Python as the programming language to develop a program that calculates the intrinsic model of the disturbed state for marine-phase soft soil. The program implementation flow is as follows:

#### (1) Relatively complete state - duncan-zhang model:

The Duncan-Zhang model is a nonlinear constitutive model for soil, suitable for describing the mechanical behavior of soil under various strain conditions. The model considers the relationship between the minimum principal stress, maximum principal stress, and strain. The calculation formula for the model is:

$$\sigma_1 = \sigma_3 + K \cdot (\sigma_3^n) \cdot \left( \frac{\varepsilon_1}{1 + R_f \cdot \frac{\varepsilon_1}{\varepsilon_f}} \right) \quad (26)$$

where  $\sigma_3$  is the minimum principal stress,  $\sigma_1$  is the maximum principal stress,  $\varepsilon_1$  is the principal strain,  $K$  is the nonlinear parameter of the soil,  $n$  is the nonlinear index,  $R_f$  is the correlation factor, and  $\varepsilon_f$  is the reference strain. The model describes the change in the soil body with strain during loading, particularly capturing the nonlinear behavior of the soil by calculating the maximum principal stress.

#### (2) Fully adjusted state - modified cambridge model:

The Modified Cambridge Model is an enhancement of the original Cambridge Model, primarily used to describe the behavior of the plastic zone in soil. This model captures the nonlinear relationship between stress and strain in the soil, accounting for the effects of strain hardening and strain softening. The calculation formula for the model is:

$$\sigma_1 = \sigma_3 + m \cdot (\sigma_1 - \sigma_3) \cdot (1 + \alpha \cdot \varepsilon_1 - \beta \cdot \varepsilon_1^2) \quad (27)$$

where  $\sigma_3$  is the minimum principal stress,  $\sigma_1$  is the maximum principal stress,  $\varepsilon_1$  is the principal strain,  $m$  is the plasticity parameter of the soil,  $\alpha$  is the strain hardening parameter, and  $\beta$  is the strain softening parameter. The model describes the transition of the soil from the elastic zone to the plastic zone during the loading process by adjusting for strain hardening and strain softening.

#### (3) Disturbance effect - based on isotropic consolidation creep test results:

The disturbance effect function is based on the dynamic changes in the soil body under different loading conditions. By calculating the disturbance effect, the nonlinear behavior of the soil under loading can be better understood. The calculation formula for the disturbance effect is:

$$\text{Disturbance Effect} = \frac{1}{1 + R_f \cdot \frac{\varepsilon_1}{\varepsilon_f}} \quad (28)$$

where  $\varepsilon_1$  is the principal strain,  $\varepsilon_f$  is the reference strain, and  $R_f$  is the correlation factor. This function is used to describe the effect of strain changes on the stresses within the soil body under varying loading conditions.

#### (4) Main program: calculation of stress-strain relationships in different states:

In the main program, the models and functions described above are called to calculate the stress-strain relationships in different states. The corresponding stress-strain curves are generated, and the data are calculated and saved simultaneously. The main program is written in Python to implement the relevant functions.

To improve readability and avoid ambiguity, the attached table summarizes all the symbols used in this manuscript.



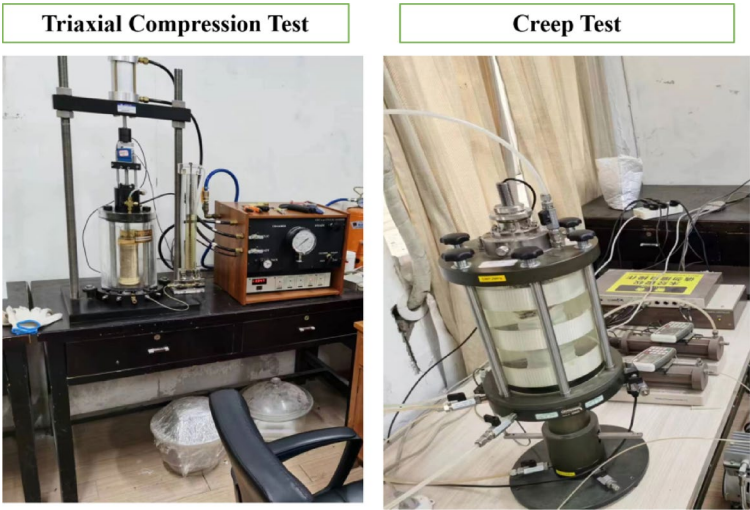


Fig. 1. Triaxial compression test and creep test.

	Depth (m)	Natural density (g/cm <sup>3</sup> )	water content (%)	Void ratio	Liquid limit (%)	Plastic limit (%)	Liquid index	Plasticity index
Sample	8.70	1.77	58.4	1.73	34	26	1.5	15.7

Table 1. Basic physical indexes of specimens.

Model validation and application  
Triaxial test for marine soft soil

To verify the accuracy of the disturbed state intrinsic model for marine-phase soft soil proposed in this thesis, a comparative analysis and validation were conducted between the test results and theoretical predictions for the stress-strain relationship of marine-phase soft soil under varying perimeter pressure conditions. This analysis was carried out using a combination of consolidation undrained triaxial tests and creep tests, as shown in Fig. 1. The marine-phase soft soil used in the tests was sampled from the Shenzhen Railway Transportation Line 12 Sea Field East Station project, and its basic physical properties are presented in Table 1<sup>21,22</sup>.

The tests were conducted following China’s Geotechnical Laboratory Test Regulations (GB/T 50123 – 1999)<sup>23</sup> and the United States’ Standard Test Method for Consolidated Drained Triaxial Compression Test for Soils (ASTM D7181-11)<sup>24</sup>. The testing equipment used in this study consists of a fully digital, pneumatic, closed-loop repetitive loading triaxial apparatus, as shown in Fig. 1. This computerized control system ensures precise control over stress or strain rate loading during the tests, with the loading process carefully regulated to maintain accuracy.

The steps for conducting the triaxial compression test are as follows:

- (1) Soil sample preparation: Soil samples are collected and placed in a well-ventilated area to air dry. This step is essential for removing excess moisture that could affect the soil’s properties. After air drying, the soil is spread on a rubber sheet and gently crushed using a wooden mallet. It is then sieved through a 2 mm aperture sieve to ensure uniformity in the soil particles, which is crucial for maintaining consistency across the tests.
- (2) Water content and compaction: The water content of the air-dried soil is measured, and the required amount of water is calculated based on the target design water contents (e.g., 40%, 45%, 50%, 55%, 60%). Water is evenly sprayed onto the soil to ensure uniform moisture distribution, and the soil is placed in a sealed plastic bag to equilibrate for 24 h. The soil is then compacted to 95% of its maximum dry density. Five specimens are prepared for each water content level, resulting in a total of 25 specimens. The mass error for each specimen is carefully controlled within ± 2 g. To prevent moisture loss and ensure stable water content, the prepared specimens are immediately wrapped in plastic.
- (3) Apply Perimeter Pressure ( $\sigma_3$ ):

Apply a predetermined perimeter pressure (e.g., 100 kPa, 200 kPa, 300 kPa) by injecting water into the pressure chamber. Open the drain valve and allow the specimen to drain and consolidate under the applied perimeter pressure until the drainage volume stabilizes (e.g., a change of less than 1% in drainage volume over 24 h). Once consolidation is complete, close the drain valve and leave the specimen undrained.

- (4) Apply axial pressure: Apply axial pressure at a constant strain rate of 1.0 mm/min.

- (5) Data recording: Record parameters such as axial stress difference ( $\sigma_1 - \sigma_3$ ), axial strain ( $\epsilon_a$ ), pore water pressure ( $u$ ), and other relevant parameters in real time.
- (6) Test termination: Terminate the test when the stress difference decreases significantly, i.e., when it reaches a stable value after the peak value.
- (7) Stress-strain curve: Based on the recorded data, plot the stress-strain curve to determine the mechanical properties of the marine-phase soft soil.

Cyclic creep tests were conducted on remolded marine soft soil specimens using a GDS-Tritech TSX servocontrolled triaxial system equipped with a 50 kN load cell (accuracy  $\pm 0.5\%$  FS) and LVDT axial and radial displacement transducers (resolution 0.001 mm). Pore pressure was measured by a pressure transducer (accuracy  $\pm 0.3\%$  FS). Data were recorded at 1 Hz. The cyclic creep test is performed as follows<sup>25</sup>:

- (1) Soil sample cutting: Five different water content levels (40%, 45%, 50%, 55%, 60%) are prepared, and soil samples are formed into specimens with a diameter of 61.8 mm and a height of 125 mm.
- (2) Backpressure saturation: The specimens undergo backpressure saturation for 12 h.
- (3) Specimen mounting: The specimen is carefully mounted in the triaxial pressure chamber to avoid disturbance. The sealed container is then prepared to begin the test.
- (4) Consolidation pressure: A consolidation pressure of 100 kPa is applied using isobaric consolidation, with drainage applied until the pore pressure dissipates.
- (5) Waveform selection: Based on the characteristics of common low-frequency cyclic loading and the working properties of the test apparatus, a trapezoidal wave cyclic loading is chosen for the clay.
- (6) Loading process: The deviator stress ratio  $q/p'$  was loaded from 0.2 to 0.6 at a constant speed, and the loading rate corresponded to the axial strain of 0.05%/min (about 0.5 kPa/s) for about 480 s. At  $q/p'=0.6$  hold for 1 200 s, the main creep is recorded. Unload  $q/p'$  from 0.6 to 0.2 at the same rate as in the loading stage, which lasts about 480 s. Hold at  $q/p'=0.2$  for 600 s for zeroing volume changes. A total of 5 cycles are applied, and the test cannot be terminated until the end of the cycle. The trapezoidal wave cyclic loading waveform, shown in Fig. 2, consists of three stages:

Stage ① and ③ are isokinetic loading and unloading phases, where the stress amplitude is applied according to the design cycle.

Stage ② represents the constant load phase. The time ratio of stages ①, ②, and ③ is set to 1/6, 4/6, and 1/6, respectively, as per the literature on low-frequency cyclic loading and creep characteristics of marine soft soil under sea accumulation.

#### Calibration of DSC model parameters from triaxial and creep tests

Use measured axial load, cell pressure, pore pressure, axial displacement, and volume change records from the triaxial program described previously. Convert axial load to total axial stress and correct for changing area; compute deviator stress  $q = \sigma_1 - \sigma_3$  and mean effective stress  $p' = (\sigma_1 + 2\sigma_3)/3$  using pore pressure data when applicable. Zero strains at the end of consolidation.

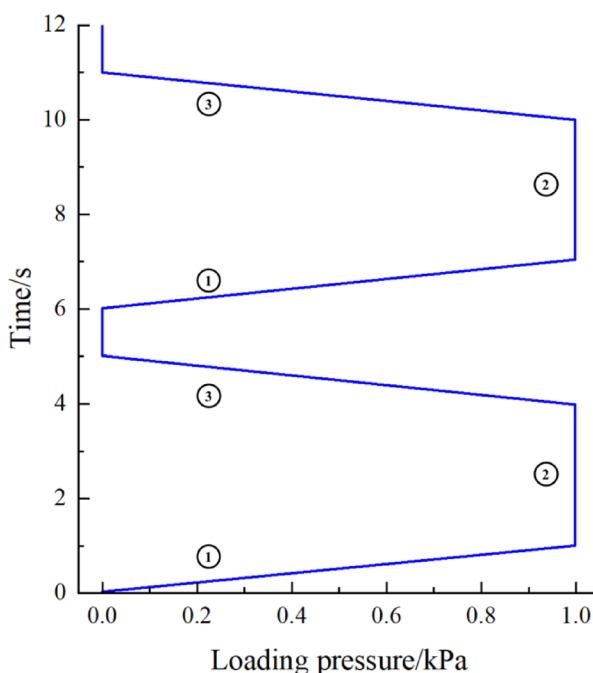


**Fig. 2.** Schematic diagram of loading for creep test.



## (1) Duncan-Zhang intactstate parameters

For each confining stress  $\sigma_3$ , compute secant modulus at 0.5% axial strain:  $E_{0.5} = (\sigma_1 - \sigma_3) / \varepsilon_a$ .

Regress  $E_{0.5} / \text{Pa} = K(\sigma_3 / \text{Pa})^n$  in logspace across all confining levels to obtain  $K$  and  $n$  (Pa = atmospheric pressure).

Determine failure point as peak  $q$  (or axial stress difference) or 15% strain if no peak; record  $(\sigma_1 - \sigma_3)_f$  and  $\varepsilon_f$ .

Compute theoretical ultimate stress difference:  $(\sigma_1 - \sigma_3)_{ult} = (\sigma_1 - \sigma_3)_f / R_f$ ; solve for  $R_f$  by nonlinear least squares minimizing residual between measured stress-strain curve and Eq. (29) below.

$$\frac{\sigma_1 - \sigma_3}{(\sigma_1 - \sigma_3)_{ult}} = \frac{R_f \varepsilon_a}{\varepsilon_f + \varepsilon_a} \quad (29)$$

Poisson's ratio  $\nu$  obtained from radial/volumetric measurements or backcomputed using Eq. (4) relationships described in the manuscript.

## (2) Modified cambridge fully adjustedstate parameters.

From 1D consolidation (oedometer) or isotropic compression path, plot void ratio  $e$  versus  $\ln p'$ .

Fit linear segments: slope of virgin compression line =  $-\lambda / (1 + e_0)$  (or  $-C_c / \ln 10$ ); slope of unloading/reload line =  $-\kappa / (1 + e_r)$  (or  $-C_r / \ln 10$ ).

Intercept at  $p' = 1$  kPa (or Pa) gives  $e_\lambda$ .

Initial void ratio  $e_0$  from specimen state at start of shearing test.

Critical state slope  $M$  from bestfit of  $q = Mp'$  through largestrain plateau points in triaxial shearing (or from friction angle relation Eq. 15).

Preconsolidation pressure  $p'_c$  taken from yield on compression curve; updated by hardening rule during shearing.

## (3) Disturbance functions from creep.

Compute time-dependent volumetric strain during constant stress isotropic creep stage; evaluate reference intact response  $\varepsilon_v^i(t)$  by integrating Duncan-Zhang with no disturbance; evaluate fully adjusted response  $\varepsilon_v^c(t)$  from MCC prediction at same stress; then compute  $D_v = (\varepsilon_v^a - \varepsilon_v^i) / (\varepsilon_v^c - \varepsilon_v^i)$  at each time increment.

Similarly for shear creep: use triaxial creep data from the trapezoidal cyclic program described in the manuscript.

Fit  $D_s$  using same normalization  $D_s = (\varepsilon_s^a - \varepsilon_s^i) / (\varepsilon_s^c - \varepsilon_s^i)$ .

**Analysis of test results**

The stress-strain relationship curves from the triaxial compression test of marine-phase soft soil are shown in Fig. 3, where the perimeter pressures are 50 kPa, 100 kPa, and 150 kPa. The data points in the figure represent the actual stress and strain values from the test. From the graphs, the following observations can be made:

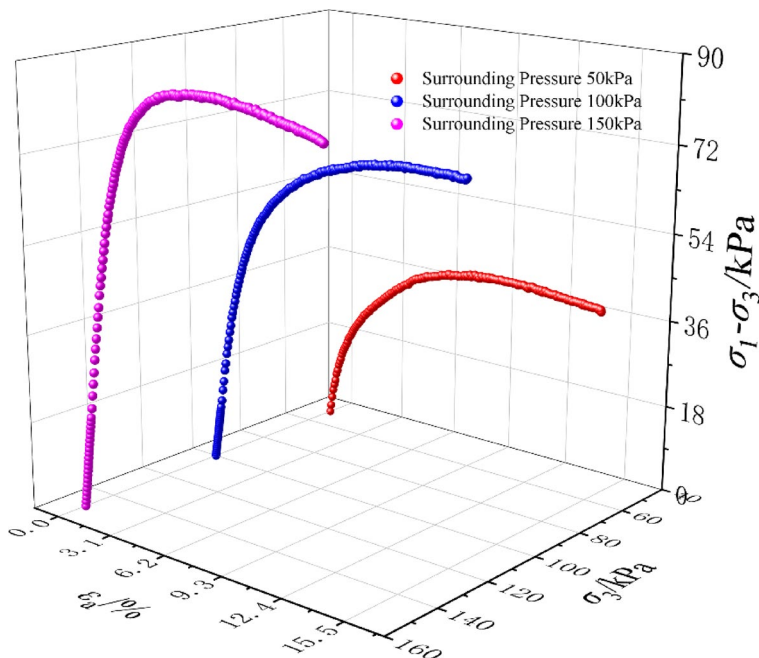


**Fig. 3.** Stress-strain relationship curve of triaxial compression test of marine soft soil.

- (1) **Effect of Perimeter Pressure on Compressive Capacity:** The compressive capacity of marine soft soil increases with the perimeter pressure, indicating that the strength and deformation characteristics of marine soft soil are closely linked to the perimeter pressure.
- (2) **Influence of Increased Perimeter Pressure:** As the perimeter pressure increases, the strength of the marine soft soil also increases, resulting in smaller deformations at the same time. The slope of the stress-strain curve decreases with higher perimeter pressure, suggesting that the compressive strength of the soil rises gradually, exhibiting greater rigidity and smaller plastic deformation.
- (3) **Deformation Behavior Under Lower Perimeter Pressure:** Under lower perimeter pressure, the strain in marine soft soil increases significantly with the applied stress, displaying more noticeable plastic deformation. As the perimeter pressure increases, the yield point of the marine soft soil shifts upward, with obvious plastic deformation occurring only at higher stress levels. This shift is important for understanding how to account for the soil's deformation characteristics under different loading conditions in engineering design.

In summary, marine-phase soft soils exhibit lower shear strengths and greater compressibility, so their mechanical behavior under varying perimeter pressures should be considered in design processes. These experimental results are valuable for evaluating soil properties in foundation treatment, subsurface structure design, and soil stability analysis, especially as the strength and deformation behavior of soils vary with changes in water depth or water table conditions.

Figure 4 presents the  $\varepsilon - t$  curve of marine soft soil under different water content conditions. From the figure, the following observations can be made:

- (1) **Creep Curve Shape and Trend:** The creep curve of marine-phase soft soil generally exhibits a trapezoidal deformation shape. The overall trend shows a gradual upward development with the extension of the cyclic loading, and this growth slows down as the stress ratio increases.
- (2) **Effect of Water Content on Axial Strain:** For the same stress ratio, the axial strain of marine-phase soft soil increases with the water content.
- (3) **Impact of High Water Content:** Marine soft soil with higher water content shows a significant increase in deformation, indicating that soils with high water content are more susceptible to deformation and damage under short-term cyclic loading.
- (4) **Strain Growth with Cyclic Cycle Extension:** As the cyclic cycle progresses, although the strain continues to increase, the rate of growth decreases in the later stages of the cycle. Eventually, the strain curve flattens and becomes horizontal, forming a trapezoidal-like pattern.

### Program implementation and performance

The Python implementation of the disturbed-state constitutive model is organized into three modules—complete\_state.py (Duncan–Zhang), adjusted\_state.py (Modified Cambridge Model), and disturbance.py—and a main script run\_dsc.py that orchestrates data I/O, solver execution, and result plotting. A high-level workflow is shown in Fig. 5.

Listing 1 shows a representative Python code snippet, please refer to the attached [Supplementary material](#).

### Verification of the accuracy of the theoretical model

To verify the accuracy of the intrinsic model of marine soft soil based on the concept of the disturbed state, the mechanical parameters of the intrinsic model were determined using the test results, as shown in Table 2. Using the calculation program for the disturbed state constitutive model, the stress-strain relationship curves of

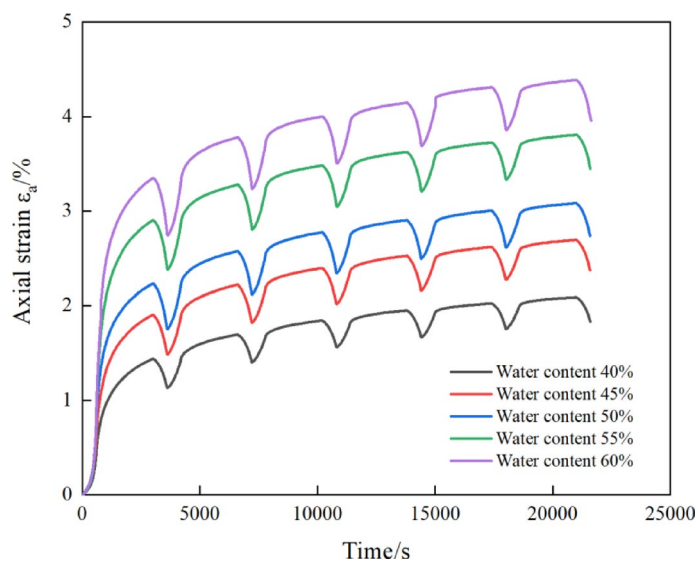


**Fig. 4.**  $\varepsilon - t$  curves of marine soft soil under different water content conditions.

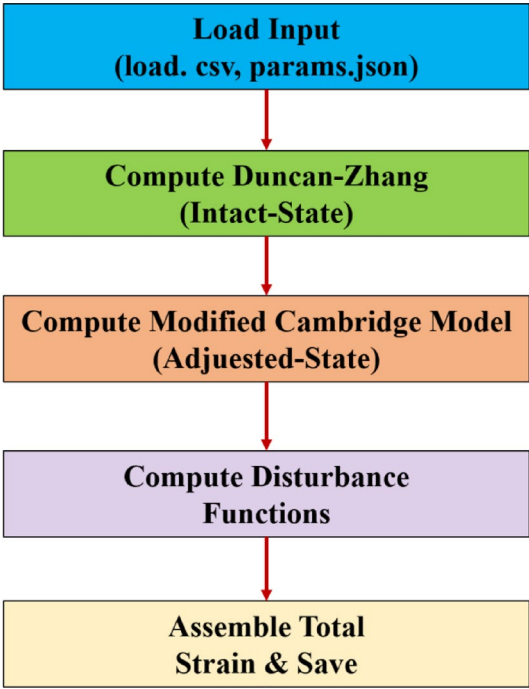


Fig. 5. Workflow of the Python implementation.

Relatively complete state		Fully adjustable status parameters			Disturbance function	
$\nu$	$E(\text{MPa})$	$\lambda$	$\kappa$	$M$	$D\nu$	$Ds$
0.3	1.24	0.16	0.07	1.10	0.4	0.4

Table 2. Experimental parameters of the intrinsic model for marine soft soils<sup>21,22</sup>.

marine soft soil under perimeter pressures of 50 kPa, 100 kPa, and 150 kPa were compared and analyzed. This comparison serves to validate the accuracy of the model.

The stress-strain relationship curves from triaxial shear tests and principal structure theory calculations for marine soft soil specimens under perimeter pressures of 50 kPa, 100 kPa, and 150 kPa are presented in Fig. 6. Figure 6 compares the disturbed-state constitutive (DSC) model predictions against laboratory data for three unconsolidated undrained (CU) triaxial tests at  $\sigma_3' = 50, 100, \text{ and } 150 \text{ kPa}$ . In all panels, black squares denote experimental deviator stress  $q = \sigma_1 - \sigma_3$  versus axial strain  $\epsilon_a$ , while the red solid line represents the DSC model response

- (1) In the low-confining-pressure test (Fig. 6(a),  $\sigma_3' = 50 \text{ kPa}$ ), the DSC model captures the overall stress-strain trend but exhibits slightly higher initial stiffness: for  $\epsilon_a < 1\%$ , the model overpredicts  $q$  by up to 10% relative to the data. The peak stress is predicted at  $\epsilon_a \approx 6.5\%$  ( $q \approx 38.5 \text{ kPa}$ ), compared with the experimental peak at  $\epsilon_a \approx 7.5\%$  ( $q \approx 39 \text{ kPa}$ ). Postpeak softening is reproduced faithfully, indicating that the disturbance functions correctly represent residual strength under low  $\sigma_3'$ .
- (2) At an intermediate confining pressure (Fig. 1(b),  $\sigma_3' = 100 \text{ kPa}$ ), the DSC model's initial stiffness and yield point align more closely with observations. The predicted and measured peaks occur at  $\epsilon_a \approx 7\%$  and  $\epsilon_a \approx 8\%$ , respectively, with  $q \approx 70 \text{ kPa}$  (model) versus  $q \approx 68 \text{ kPa}$  (experiment). Beyond  $\epsilon_a > 10\%$ , the model slightly overestimates residual strength, suggesting that the shear disturbance exponent  $Z_s$  may be marginally over-predicted for this  $\sigma_3'$  level.
- (3) Under high confining pressure (Fig. 1(c),  $\sigma_3' = 150 \text{ kPa}$ ), the model achieves excellent agreement across the entire strain range. Initial tangent modulus, peak stress ( $q \approx 88 \text{ kPa}$  at  $\epsilon_a \approx 7.5\%$ ), and postpeak plateau remain within 5% of experimental values. This close match demonstrates that the combined Duncan–Zhang stiffness parameters ( $K, n$ ), Modified CamClay indices ( $\lambda, \kappa, M$ ), and disturbance coefficients ( $A_p, Z_p, A_s, Z_s$ ) converge to optimal values under elevated  $\sigma_3'$  conditions.

Overall, these results confirm that the DSC model reliably reproduces key features of marine soft soil behavior across a spectrum of confining pressures. The slight early peak predicted at lower  $\sigma_3'$  suggests a targeted recalibration of the failure strain parameter  $\epsilon_p$ , whereas minor overprediction of residual strength at  $\sigma_3' =$

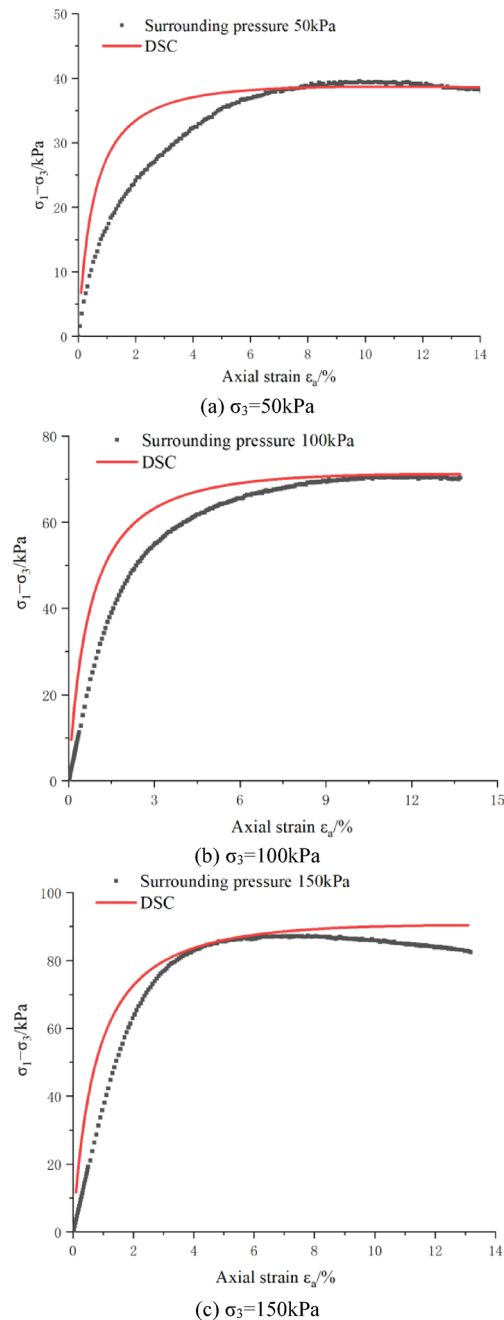


**Fig. 6.** Comparative analysis of stress-strain relationship curves of marine soft soil specimens.

100 kPa indicates scope for refining the shear disturbance exponent. Such sensitivity-guided adjustments will further enhance the model's predictive accuracy in practical geotechnical applications.

### Application of theoretical model

A temporary stacked municipal building concrete structure located in a marine-phase soft soil area in Shenzhen City, with a length of 10 m, was subjected to different homogeneous pressures relative to the surface of the marine-phase soft soil layer. To explore the applicability of the theoretical model, a two-dimensional simplified model for foundation settlement was established using the ABAQUS finite element program. The model is 60 m long and 40 m high, composed entirely of marine-phase soft soil layers.

To ensure consistency with the DSC calibration, we derive the Mohr–Coulomb parameters directly from the DSC-fitted values. The friction angle  $\phi_{MC}$  is obtained from the critical state parameter  $M$  via

$$M = \frac{6 \sin \phi_{MC}}{3 - \sin \phi_{MC}} \Rightarrow \phi_{MC} = \arcsin\left(\frac{3M}{6 + M}\right) \quad (30)$$

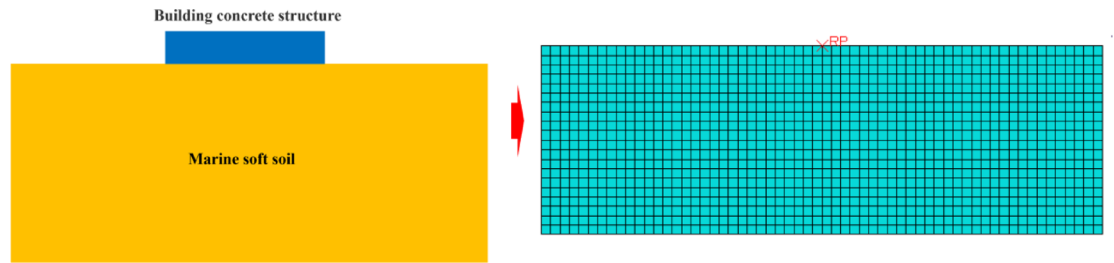


**Fig. 7.** Numerical calculation model.

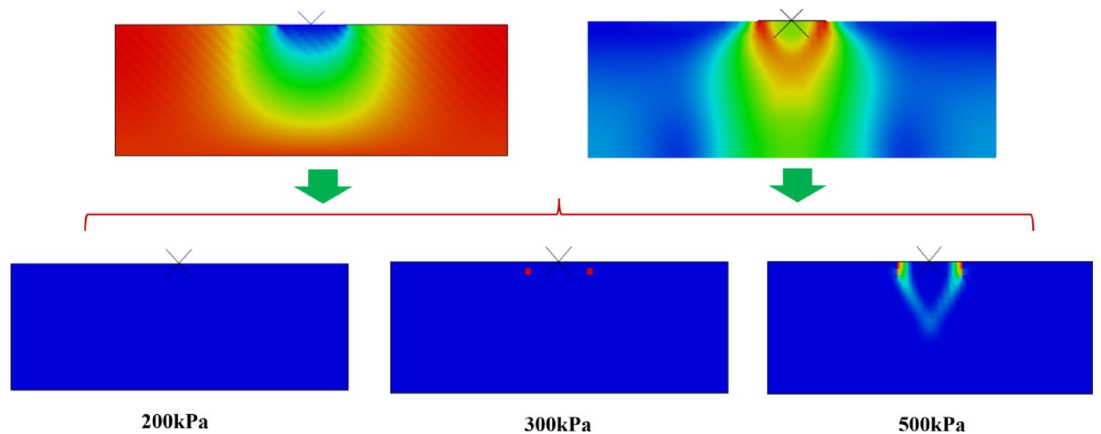


**Fig. 8.** Cloud diagram of stress-strain and equivalent plastic strain induced by concrete structure of municipal building with temporary pile load in marine soft ground layer.

Cohesion  $c_{MC}$  is then determined by fitting the M-C yield envelope to the DSC-predicted peak deviator stresses  $q_f$  at three confining pressures ( $\sigma_3' = 50, 100, 150$  kPa) by minimizing

$$\sum_i (q_{f,i} - [2c_{MC} \cos \phi_{MC} + 2\sigma_3 \sin \phi_{MC}])^2 \quad (31)$$

Finally, the elastic modulus  $E_{MC}$  and Poisson's ratio  $\nu_{MC}$  are set equal to the DSC small-strain values  $E_{0.5}$  and  $\nu$  at 0.5% axial strain, ensuring identical initial stiffness. These consistent parameter linkages isolate the constitutive differences between the Mohr-Coulomb and DSC formulations in the comparative analysis.

So, the intrinsic model used for the soil is the Mohr-Coulomb Model, with the following mechanical parameters: an internal friction angle of  $10^\circ$ , cohesion of 11 kPa, an elasticity modulus of 1.26 MPa, and a Poisson's ratio of 0.3, as shown in Fig. 7. The municipal building concrete structure is modeled as a rigid structure acting on the marine soft soil layer, with applied loads of 200 kPa, 300 kPa, and 500 kPa at its reference point (RP) to simulate the effect of the temporary stacked municipal building on the settlement of the marine soft soil layer. Among them, With the center of the structure as the origin, it extends 20 m on the left and right, and 40 m down from the surface, and the bottom is regarded as a fixed surface. The marine soft soil adopts CPE4R (4-node bilinear planar strain unit, reduction integral). The horizontal displacement ( $U_x = 0$ ) is fixed on both sides of the vertical plane to prevent the overall translation. The bottom surface is fixed with horizontal and vertical displacement ( $U_x = U_y = 0$ ) to simulate deep soil support.

Figure 8 presents the cloud diagram of stress-strain and equivalent plastic strain in the marine soft soil layer induced by the concrete structure of the temporary pile-loaded municipal building. From the figure, the following observations can be made:

- (1) **Strain Behavior:** The strain trend of the marine soft soil layer under different loads is consistent, with only the deformation values differing. The maximum settlement occurs at the contact point between the concrete structure of the temporary pile-loaded municipal building and the marine soft soil. The maximum settlement and deformation values are as follows:

Under a 200 kPa load: 1.27 cm.  
 Under a 300 kPa load: 1.89 cm.  
 Under a 500 kPa load: 3.52 cm.

Temporary load	200 kPa	300 kPa	400 kPa	500 kPa	600 kPa
Numerical calculation	109.37 kPa	149.02 kPa	189.14 kPa	228.86 kPa	267.88 kPa
DSC	106.29 kPa	145.81 kPa	185.85 kPa	225.92 kPa	264.92 kPa
Difference between calculated values	2.82%	2.15%	1.74%	1.28%	1.10%

**Table 3.** Gives a comparison of the maximum stress values calculated by the numerical calculation at the reference point with those calculated by the disturbed state constitutive model. From the table, it can be seen that: (1) the maximum stress values obtained from the ontological model of marine soft soil based on the concept of disturbed state are smaller than those based on the numerical calculation of ABAQUS. (2) the maximum stress values obtained by this method do not differ much, and the errors are within 3%. To summarize, the intrinsic model of marine soft soil based on the concept of disturbed state can be used to evaluate the performance of foundation bearing capacity of marine soft soil layer.

(2) **Stress Behavior:** The stress trend of the marine soft soil layer under different loads is also consistent, with only the stress values differing. The maximum stress occurs at the contact point between the concrete structure and the marine soft soil. The maximum stress values are as follows:

Under a 200 kPa load: 109.37 kPa.  
Under a 300 kPa load: 149.02 kPa.  
Under a 500 kPa load: 228.86 kPa.

(3) **Shear Deformation and Damage:** As the temporary pile load increases, the contact area between the soft soil and the concrete structure experiences gradual shear deformation damage, ultimately leading to penetration damage. For this reason, the lower 1.00 m of the contact area between the center point of the concrete structure of the municipal building and the marine soft soil is selected as the reference point. The calculated values from the constitutive model proposed in the paper are then compared and analyzed.

**Table 3.** Comparison of maximum stress values calculated by numerical calculations and disturbed state eigenmodel calculations.

**Discussion of design implications**

Although the peak deviator stress predicted by the DSC model differs from that of the conventional Mohr–Coulomb (M–C) model by less than 3%, it is important to assess the practical significance of this discrepancy in key design contexts: settlement prediction, bearing-capacity and structural safety.

**Impact on settlement prediction**

In soft-soil foundation design, long-term settlement is typically estimated using either the compression-index method or constitutive-integration approaches. For the former, the settlement *s* is given by:

$$s = \frac{\Delta\sigma_v C_c}{1 + e_0} \ln \frac{\sigma_{v,0} + \Delta\sigma_v}{\sigma_{v,0}} \tag{32}$$

where  $\Delta\sigma_v$  is the additional vertical effective stress,  $C_c$  the compression index,  $e_0$  the initial void ratio, and  $\sigma_{v,0}$  the initial vertical effective stress. A 3% difference in model-predicted peak stress translates to a 3% difference in  $\Delta\sigma_v$ . For example, with  $\sigma_{v,0} = 100$  kPa and  $\Delta\sigma_v \approx 100$  kPa, and taking  $C_c = 0.3$  and  $e_0 = 1.2$ , the resulting settlement variation is.

$$\Delta s \approx \frac{3\text{kPa} \times 0.3}{1 + 1.2} \ln \frac{200 + 3}{200} \approx 1.5\text{mm}$$

Given that a typical design settlement margin is 20–100 mm, this equates to only 1.5–7.5% of the total amount, while the design code typically allows for tolerances of 5–10%.

**Bearing capacity and structural safety**

Ultimate bearing capacity  $q_u$  in foundation design is related to the factor of safety ( $F_s$ ) by:

$$q_{\text{design}} = \frac{q_u}{F_s} \tag{33}$$

Adopting  $F_s = 1.4$  and assuming  $q_u = 300$  kPa, a 3% variation in  $q_u$  yields:

$$q_{\text{design}}^{\text{DSC}} = \frac{300}{1.4} \approx 214.3\text{kPa}, \quad q_{\text{design}}^{\text{DSC}} = \frac{291}{1.4} \approx 207.9\text{kPa}$$

a mere 6.4 kPa difference ( $\approx 3\%$ ). Such a small shift in design capacity has negligible effect on foundation type selection or pile layout, and falls well within the safety margins provided by standard second-check procedures.



In summary, although there is a small difference between the DSC model and the traditional M–C model in the prediction of deviator stress, the deviation falls within the allowable error range of the code in the two core decision-making links of settlement control and bearing capacity design, and will not lead to the fundamental adjustment of the engineering scheme. On the contrary, the DSC model has significant advantages in simulating the nonlinear strength softening, creep coupling and disturbance effects of soft soils, which can provide more refined predictions under more complex loads-deformation histories, and improve the reliability and economy of engineering design.

## Conclusion

Marine soft soil is widely distributed in near-coastal areas and, due to its unique mechanical properties, is highly prone to deformation and destabilization, especially for marine structures built on it. Although extensive research has been conducted both domestically and internationally on the mechanical properties of marine soft soil through various constitutive models, no attempts have been made to develop a mechanical model based on the concept of disturbed state for marine soft soil.

In response, this paper proposes a novel approach based on the disturbed state concept. It uses the Duncan tensor modulus to describe the relatively intact state of marine soft soil, the modified Cambridge model to characterize the fully adjusted state, and a creep test to derive the disturbance function for marine soft soil. These elements are combined to establish an intrinsic model of the disturbed state for marine soft soil. The model is verified through relevant tests and applied to engineering case studies.

The comparative analysis shows that the proposed disturbed state constitutive model effectively assesses the foundation bearing capacity of marine soft soil. This method offers a new theoretical framework and calculation approach for studying the mechanical properties of marine soft soil in near-coastal regions.

## Data availability

The research data of the paper can be obtained by email corresponding author.

Received: 13 February 2025; Accepted: 8 August 2025

Published online: 13 August 2025

## References

- Jostad, H. P. & Yannie, J. A procedure for determining long-term creep rates of soft clays by triaxial testing. *Eur. J. Environ. Civil Eng.* **26** (7), 2600–2615 (2022).
- LIN Dong. Constitutive model for compression behavior of marine silt soft clay and its application. *Railway Constr. Technology*, (10):1–5. (2023).
- Baojun, L. I., Weijun, H. U. A. N. G. & Pengjun, Z. H. A. N. G. Experimental study on cumulative plastic strain of marine soft soil under cyclic loading. *Mod. Tunn. Technol.* **57** (S1), 780–786 (2020).
- Qiangfei. Study on constitution model of loess based on disturbed state concept[D]. *Doctoral Thesis of Chang'an University*, (2016).
- Huang, M. S., Zou, S. H., Shi, Z. H. & Hong, Y. Constitutive modeling of cyclically loaded clays with entrapped gas bubbles under undrained and unexhausted conditions. *Acta Geotech.* **18** (1), 265–278 (2023).
- Wang, Y. K. et al. Study on fractional-order elastic-plastic constitutive model of river silt based on critical state theory. *Mar. Georesources Geotechnol.* **42** (1), 59–66 (2024).
- Ai, Z. Y., Yuan, J. T., Zhao, Y. Z. & Dai, Y. C. Viscoelastic-viscoplastic damage analysis of transversely isotropic soft soils. *Eng. Geol.* **310**, 106878 (2022).
- Yuan, Y., Liu, R., Fu, D. F. & Sun, G. D. Secondary development and application of structural marine clay damage model. *Rock. Soil. Mech.* **43** (7), 1989–2002 (2022).
- Hong, Y., Wang, X. T., Wang, L. Z. & Gao, Z. W. A state-dependent constitutive model for coarse-grained gassy soil and its application in slope instability modelling. *Comput. Geotech.* **129**, 103847 (2021).
- Yan, T. C. et al. Mechanical characteristics and damage constitutive model of Fiber-Reinforced Cement-Stabilized soft clay. *Appl. Sci. -Basel.* **14**, 1378 (2024).
- Chen, Z. J. & Yin, J. H. A new One-Dimensional thermal Elastic-Viscoplastic model for the thermal creep of saturated clayey soils. *J. Geotech. Geoenviron. Eng.* **149** (4), 1847–1862 (2023).
- Desai, C. S. et al. A consistent finite element technique for work-softening behaviour[C]. In *Proceedings of the International Conference on Computation Methods in Nonlinear Mechanics*, Austin, Oden (eds), (1974).
- Desai, C. S. Constitutive modelling using the disturbed state as microstructure self-adjustment concept. In *Continuum Models of Materials with Microstructure*, Muhlhaus (ed.) ; 239–296. (1995).
- Xu, Y. L. et al. Modelling the triaxial compression behavior of loess using the disturbed state concept. *Adv. Civil Eng.*, 6638715. (2021).
- Wu, Z. P., Xu, J., Li, Y. F. & Wang, S. H. Disturbed state Concept-Based model for the uniaxial Strain-Softening behavior of Fiber-Reinforced soil. *Int. J. Geomech.* **22** (7), 1546–1562 (2022).
- Ouria, A. Coupled creep and nonlinear consolidation of soft soils in disturbed state concept framework. *Comput. Geotech.* **166**, 105955 (2024).
- Zhang, C., Zhou, X. & Lu, J. Modified constitutive model of sandy pebble soil based on disturbed state concept. *Arab. J. Geosci.* **15**, 587 (2022).
- Desai, C. S., Basaran, C. & Zhang, W. Numerical algorithm and mesh dependance in the disturbed state concept. *Int. J. Numer. Methods Eng.* **40** (16), 3059–3083 (1997).
- WU Gang. Disturbed state constitution models of engineering material (I)-Disturbed state concept and its theory principium. *Chin. J. Rock Mechan. Eng.* **21** (6), 759–765 (2002).
- WU Gang. Disturbed state constitution model of engineering material (II)-DSC-based numerical simulation of finite element method. *Chin. J. Rock Mechan. Eng.* **21** (8), 1107–1110 (2002).
- Wenbin, X. I. A. O. et al. Experiment and analysis on dynamic characteristics of marine soft clay. *Mar. Georesources Geotechnol.* <https://doi.org/10.1080/1064119X.2024.2351172> (2024).
- Wu ke, X. U. et al. Mechanical properties of marine soft soil and its influence on urban underground track transport engineering. *J. Water Resour. Architectural Eng.* **22** (2), 122–131 (2024).
- GB/T50123-. ; Standard for Geotechnical Testing Method[S]. *National Standard of the People's Republic of China: Beijing, China*, 2019. 21. (2019).

24. ASTM D7181-11. Method for Consolidated Drained Triaxial Compression Test for Soils[S]. *American Society for Testing and Materials: Conshohocken*, PA, USA, (2011).
25. Wenbin, X. U., Ke, W. U., Wenbin, X. I. A. O., Yajun, L. I. U. & Rong, C. H. E. N. Experimental study on creep characteristic of remolded marine soft soil under Cyclic loading. *Eng. Technol. Res.* **23**, 15–18 (2024).

## Acknowledgements

This work was supported by National Natural Science Foundation of China (52179106).

## Author contributions

K.W., H.J.L. and R.C. conceived the experiment(s), H.Z. and Y.D.S. conducted the experiment(s), Y.J.L. and Y.Z. analysed the results; K.W. and H.Z. wrote the main manuscript text. All authors reviewed the manuscript.

## Declarations

## Competing interests

The authors declare no competing interests.

## Additional information

**Supplementary Information** The online version contains supplementary material available at <https://doi.org/10.1038/s41598-025-15607-3>.

**Correspondence** and requests for materials should be addressed to K.W.

**Reprints and permissions information** is available at [www.nature.com/reprints](http://www.nature.com/reprints).

**Publisher's note** Springer Nature remains neutral with regard to jurisdictional claims in published maps and institutional affiliations.

**Open Access** This article is licensed under a Creative Commons Attribution-NonCommercial-NoDerivatives 4.0 International License, which permits any non-commercial use, sharing, distribution and reproduction in any medium or format, as long as you give appropriate credit to the original author(s) and the source, provide a link to the Creative Commons licence, and indicate if you modified the licensed material. You do not have permission under this licence to share adapted material derived from this article or parts of it. The images or other third party material in this article are included in the article's Creative Commons licence, unless indicated otherwise in a credit line to the material. If material is not included in the article's Creative Commons licence and your intended use is not permitted by statutory regulation or exceeds the permitted use, you will need to obtain permission directly from the copyright holder. To view a copy of this licence, visit <http://creativecommons.org/licenses/by-nc-nd/4.0/>.

© The Author(s) 2025